Mechanism of platelet adhesion to von Willebrand factor and microparticle formation under high shear stress

Armin J. Reininger, Harry F. G. Heijnen, Hannah Schumann, Hanno M. Specht, Wolfgang Schramm, and Zaverio M. Ruggeri

We describe here the mechanism of platelet adhesion to immobilized von Willebrand factor (VWF) and subsequent formation of platelet-derived microparticles mediated by glycoprotein Ibα (GPIbα) under high shear stress. As visualized in whole blood perfused in a flow chamber, platelet attachment to VWF involved one or few membrane areas of 0.05 to 0.1 μm^2 that formed discrete adhesion points (DAPs) capable of resisting force in excess of 160 pN. Under the influence of hydrodynamic drag, membrane tethers developed between the moving platelet body and DAPs firmly adherent to immobilized VWF. Continued stretching eventually caused the separation of many such tethers, leaving on the surface tube-shaped or spherical microparticles with a diameter as low as 50 to 100 nm. Adhesion receptors (GPIbα, αIIbβ3) and phosphatidylserine were expressed on the surface of these microparticles, which were procoagulant. Shearing platelet-rich plasma at the rate of 10 000 s^{-1} in a cone-and-plate viscosimeter increased microparticle counts up to 55-fold above baseline. Blocking the GPIb-VWF interaction abolished microparticle generation in both experimental conditions. Thus, a biomechanical process mediated by GPIbα-VWF bonds in rapidly flowing blood may not only initiate platelet arrest onto reactive vascular surfaces but also generate procoagulant microparticles that further enhance thrombus formation. (Blood. 2006;107:3537-3545)

Introduction

The integrity of the vessel wall is key for the normal circulation of blood and is constantly surveyed by platelets.[1] In arterial flow, platelets are positioned at high density near the endothelial-cell layer, while erythrocytes are lifted away from it through a hemodynamic process called axial migration.[2,3] When damage to the vascular surface occurs, von Willebrand factor (VWF) binds rapidly to exposed subendothelial structures[4,5] and enables platelet arrest from fast-flowing blood through the interaction of its A1 domain (VWFA1) with the platelet glycoprotein Ibα (GPIbα) receptor.[6] The VWFA1-GPIbα bond has a short half-life and by itself cannot provide irreversible adhesion. Consequently, the torque imposed by flowing blood causes platelets to translocate over immobilized VWF until receptors such as glycoprotein VI or integrin αIIbβ3 engage their respective ligands and mediate permanent adhesion, spreading, and aggregation.[7] Under the effect of shear stress, platelet-derived microparticles (PMPs) can be generated in blood through a process that was reported to be dependent on the VWF-GPIbα interaction by some investigators[8] but not others.[9] Owing to their ability to bind coagulation factors, and the exposure on their surface of phosphatidylserine[9] as well as adhesion receptors[10] and possibly tissue factor,[11,12] PMPs have been suggested to play a role in blood clotting and thrombus formation.[13] Lacking so far, however, is a direct visualization and explanation of how shear stress can induce the generation of microparticles from platelets and how this may be linked to the subsequent development of thrombi. Because fast-flowing blood can rapidly dilute any procoagulant activity in the fluid phase, a mechanism to explain these phenomena should account not only for how microparticles are formed but also how they can be at functionally effective concentrations in areas of the circulation where wall shear rates (γ_w) can exceed 40 000 s^{-1} such as in stenosed coronary arteries.[14-16] Here, we report the results of ex vivo flow experiments using reflection interference contrast videomicroscopy (RICM)[17,18] in real time, which visualize in greater detail than available to date the mechanisms that support the initial GPIbα-mediated contact with immobilized VWF. Moreover, we demonstrate how this adhesive interaction leads to the formation of platelet membrane tethers under the influence of elevated shear stress, and how this process eventually generates microparticles that remain adherent to the VWF surface. Finally, we show that shear stress can induce PMP generation through a mechanism entirely dependent on GPIbα-VWF bonding also in a cone-and-plate viscosimeter, in the absence of interaction with immobilized VWF, and that such microparticles are highly procoagulant.

From the Department of Transfusion Medicine and Hemostaseology, Clinic for Anesthesiology, University Clinic Munich, Ludwig-Maximilians-University, Munich, Germany; the Department of Hematology, Division of Thrombosis and Hemostasis, University Medical Center Utrecht, Utrecht, the Netherlands; the Department of Cell Biology, University Medical Center Utrecht, Utrecht, the Netherlands; and the Roon Center for Arteriosclerosis and Thrombosis, Division of Experimental Hemostasis and Thrombosis, Department of Molecular and Experimental Medicine, The Scripps Research Institute, La Jolla, CA.

Submitted February 14, 2005; accepted December 19, 2005. Prepublished online as *Blood* First Edition Paper, January 31, 2006; DOI 10.1182/blood-2005-02-0618.

Supported by the National Institutes of Health (grants HL31950, HL42846, and HL78784) (Z.M.R.), the Deutsche Forschungsgemeinschaft (grant Re-1293/3-1) (A.J.R.), the Friedrich-Baur-Stiftung (A.J.R.), and Förderprogramm Forschung und Lehre, Medical Faculty, Ludwig-Maximilians-University Munich (grant Reg.-Nr. 33./2003) (A.J.R. and H.S.).

The online version of this article contains a data supplement.

An Inside *Blood* analysis of this article appears at the front of this issue.

Reprints: Armin J. Reininger, Department of Transfusion Medicine and Hemostaseology, University Clinic Munich, Ziemssenstr. 1, 80336 Munich, Germany; e-mail: armin.reininger@med.uni-muenchen.de.

The publication costs of this article were defrayed in part by page charge payment. Therefore, and solely to indicate this fact, this article is hereby marked "advertisement" in accordance with 18 U.S.C. section 1734.

Materials and methods

Preparation of blood

Blood drawn from an antecubital vein was collected into appropriate anticoagulants, either 0.106 M trisodium citrate, 1.6 mg/mL EDTA, or the thrombin inhibitor D-phenylalanyl-L-prolyl-L-arginine chloromethyl ketone dihydrochloride (PPACK; 93 μM; Hematological Technologies, Essex Junction, VT).[19] When indicated, prostaglandin E_1 (PGE_1; 10 μM; Sigma Chemical, St Louis, MO), EDTA (5 mM), and apyrase (1.5 ATPase U/mL; Sigma) were added to the blood containing PPACK. All anticoagulants gave the same results with regard to PMP and tether formation. To perform experiments in the absence of plasma proteins, blood cells were washed in modified Tyrode buffer as reported previously.[7,19] For flow experiments, the platelet count in the washed cell suspension was adjusted to the original value in blood (230 000-390 000/μL) or to 11 000/μL, the latter to reduce the number of events on the surface and to facilitate image analysis. Platelet-rich plasma (PRP) and platelet-poor plasma (PPP) were obtained by centrifuging blood for 15 minutes at 170*g* and 1070*g*, respectively. To avoid the activating effect of the washing procedure, selected experiments in the flow chamber and cone-and-plate viscosimeter were conducted with whole blood. All studies involving human subjects were conducted in accordance with the Declaration of Helsinki following protocols approved by the institutional review boards for the Scripps Research Institute and the University Clinic Munich. Informed consent to participate in the studies was obtained from all subjects.

Real-time visualization of platelet adhesion and microparticle formation

Perfusion experiments were conducted at 37°C using as substrates immobilized multimeric VWF, recombinant dimeric (d) VWFA1, or fibrillar type I collagen either from bovine tendon (acid insoluble; Sigma) or equine tendon (Horm-Chemie; Nycomed, Munich, Germany) coated onto glass coverslips used to assemble a parallel plate rectangular flow chamber.[6,7] Plasma VWF was purified as previously described.[20] Recombinant dVWFA1 was purified from the culture medium of transfected *Drosophila melanogaster* cells. This homodimeric fragment (mature residues 445-733) comprises part of the D3 domain, with interchain disulfide bonds as in plasma VWF,[21] and the entire A1 domain. Cytochalasin D (final concentration, 4 μM; Sigma) dissolved in DMSO was added to anticoagulated blood or PRP 10 minutes before the experiment. A syringe pump (Harvard Apparatus, Boston, MA) was used to aspirate blood at the desired flow rate through the chamber mounted on the stage of either an inverted microscope (Axiovert 135M; Carl Zeiss, Germany) or an upright microscope (Axioskop 2 plus; Carl Zeiss). Reflection interference contrast microscopy (RICM) was performed using a Plan-Neofluar 63 ×/1.25 Oil Ph3 Antiflex objective (Carl Zeiss) and a 50-W mercury lamp for illumination. This technique, which does not require labeling of the cells, resolves the contact area between cell membrane and adhesive surface, indicating the separation distance through interference colors.[17,18] In our studies, light reflected from the substrate-coated glass surface interfered with that reflected from the membrane of platelets flowing in close proximity to or interacting with it. Because we used a black-and-white video camera, interference colors were obtained on a gray scale in which zero-order black corresponds to a separation between 2 surfaces of 4 to 12 nm and white to more than 20 to 30 nm.[17,18] Structures separated by more than 30 nm appear as out of focus. All experiments were recorded on S-VHS videotape using a CCD camera and VCR (DXC-390 and SVO-9500MD, respectively; Sony, Inchinomiya, Japan) at the acquisition rate of 30 frames s^{-1}. Image analysis was performed off-line using Metamorph (Universal Imaging, West Chester, PA).[6] The movies, available at the *Blood* website as supplemental material (click on the Supplemental Movies link at the top of the online article) were prepared with Adobe Premiere (Adobe Systems, San Jose, CA).

Confocal microscopy analysis of tethers and PMPs

Tether and microparticle formations were fast, flow-dependent processes that required an adaptation of specimen fixation for detailed microscopic analysis. Tethers and PMPs that transiently adhered to dVWFA1 or VWF were rapidly perfusion-fixed, without interrupting flow, with a buffered 2% glutaraldehyde or 4% paraformaldehyde solution (Serva, Heidelberg, Germany). This literally "froze" platelets, tethers, and PMPs during their motion over the surface. After 10 minutes the aldehyde was removed with 3 successive washes using phosphate-buffered saline (PBS; pH 7.4). For laser scanning confocal microscopic analysis, the specimens were incubated with primary monoclonal antibodies (mAbs) for 1 hour at room temperature, followed by 1-hour incubation with fluorescence-labeled secondary antibodies. mAbs against CD41 (integrin αIIb), CD42a (GPIbα), or CD14 (monocyte marker) were from Immunotech (Marseille, France), and the mAb against tissue factor was from American Diagnostica (Stamford, CT). mAb AK-3 (anti-GPIbα, IGg1) was kindly provided by M.C. Berndt (Prahan, Australia). Rhodamine-conjugated phalloidin was from Pharmingen (Becton Dickinson, San Jose, CA). Antiactin mAb (clone 4) was from ICN Biomedicals (Irvine, CA). FITC- and Cy3-conjugated secondary antibodies were from Nordic (Tilburg, The Netherlands) and Jackson (West Grove, PA), respectively. After washing off the antibodies with PBS, specimens were mounted with Entellan on glass slides (Merck, Darmstadt, Germany) and examined with a LSM 510 Meta (Carl Zeiss) using either the Zeiss 63 × Antiflex or the Plan-Apochromat 63 ×/1.4 oil DIC objectives. For analysis of the F-actin content, fixed specimens were permeabilized with 0.2% Triton-X-100 and incubated for 1 hour with antiactin mAb followed by Cy3-labeled rabbit antimouse antibody or with TRITC-conjugated phalloidin.

Electron microscopy of platelets, tethers, and PMPs

Scanning electron microscopy (EM) was performed with a JSM-6300F instrument (JEOL, Tokyo, Japan). Fixed specimens were dehydrated in a series of ethanol baths with concentration increasing up to 100% and then critical-point dried with CO_2 and sputter-coated with platinum. For immuno-EM analysis, we prepared whole mounts and thin frozen sections of dVWFA1-bound platelets and tethers. Whole mounts were obtained by placing carbon-coated formvar grids in the perfusion chamber. After perfusion fixation with a mixture of 2% paraformaldehyde and 0.2% glutaraldehyde in 0.1 M sodium phosphate buffer, the grids with bound platelets and tethers were incubated with primary antibodies followed by protein A coupled with 10 nm gold particles. For ultrathin cryosectioning, perfusion was carried out on melamine-coated glass coverslips[22] onto which dVWFA1 was immobilized. After perfusion fixation, the melamine film with adherent platelets, tethers, and PMPs was detached from the glass, embedded in 10% gelatin, cooled in ice, and cut into 1-mm^3 blocks. The blocks were infused with 2.3 M sucrose at 4°C for 24 hours, frozen in liquid nitrogen, and stored until cryo-ultramicrotomy. Fifty-nanometer thick cryosections were cut at −120°C, using an Ultracut S ultramicrotome (Leica, Reichert Division, Vienna, Austria), collected on carbon-coated formvar grids and incubated with primary antibodies followed by protein A coupled with 10-nm gold particles. Immunolabeled whole mounts and cryosections were counterstained with uranyl acetate, embedded in methyl cellulose–uranyl acetate, and viewed in a JEOL 1200CX electron microscope.

Shearing in a cone-and-plate viscosimeter

PRP was subjected to shear rates of 10 s^{-1}, 2000 s^{-1}, 6000 s^{-1}, or 10 000 s^{-1} in a cone-and-plate viscosimeter with 0.5° cone angle and 26 μm cone-plate distance (Haake Rheovisco 1, Thermo Electron Corporation, Waltham, MA) in the absence of erythrocytes to avoid hemolysis. In selected experiments, integrin αIIbβ3 was blocked with 8 μM tirofiban (MSD Sharp & Dohme, Haar, Germany), platelet activation with PGE_1 and apyrase, and the GPIbα-VWF interaction with NMC-4 Fab, a function-blocking antibody (see "Procoagulant function of PMPs generated by platelet exposure to high shear stress"). We also used corn trypsin inhibitor (CTI; Calbiochem, La Jolla, CA) to test the effect of blocking the contact activation of clotting on PMP count and annexin V exposure. The generation of PMPs in sheared PRPs was evaluated using flow cytometry (Coulter Epics XL; Beckman Coulter, Krefeld, Germany). Platelets and microparticles were labeled with mAbs against CD41, CD42a, CD14, tissue

factor, or annexin V (PE-Cy5; Biovision, Mountain View, CA). Because of the small microparticle size, with diameter as low as 0.1 μm, detection was triggered with the fluorescence signal rather than forward scatter. We could not obtain reliable flow cytometric results for microparticles double-labeled with fluorochromes that show extensive overlap of their emission spectra in measuring channels FL1 and FL2 (eg, FITC and PE). Only combining FITC with PE-Cy5, which are measured in channels FL1 and FL4, allowed double-staining. Thus, in experiments using FITC and PE the microparticles could only be indirectly cross-referenced with respect to size and expression of tissue factor, CD41, or CD42a. Microparticles bearing a specific fluorescence signal were counted over a 1-minute acquisition period. Size calibration (forward scatter) was performed using Alexa-488–labeled microspheres with a diameter of 0.1 μm (Molecular Probes Europe, Leiden, The Netherlands).

Measurement of PMP-enhanced thrombin generation

Thrombin generation measurements in sheared PRP were performed with an automated random access coagulation analyzer (ACL 9000; Instrumentation Laboratory [IL], Barcelona, Spain). Optical signals were detected at a wavelength of 405 nm. Coagulation was initiated using either 25 mM $CaCl_2$ alone or in combination with low concentrations of recombinant tissue factor (1.44 ng/mL, PT reagent Recombiplastin; IL) dissolved in barbitone buffer (pH 7.4; Diagnostica Stago, Asnières sur Seine, France). Platelets and PMPs from sheared samples served as a source of phospholipids. Thrombin formation was detected using the chromogenic substrate, H-D-CHG-Ala-Arg-pNa·2AcOH (K_M = 15.9 μM), at the concentration of 250 μM (Pentapharm, Basel, Switzerland). The time of maximal velocity of substrate conversion was taken as the clotting time. Fibrin polymerization in the sample was inhibited using a fibrin polymerization inhibitor (H-Gly-Pro-Arg-Pro-OH·AcOH; Pentapharm). Statistical analyses were performed using the Student *t* test.

Results

Platelet attachment to VWF occurs through discrete adhesion points

At γ_w ranging from 50 s^{-1} to 40 000 s^{-1}, platelets always arrested from flowing blood onto immobilized VWF multimers by interaction of discrete adhesion points (DAPs) of the cell membrane, each with an area of 0.05 to 0.25 μm^2 (Figure 1A; Supplemental Movie S1). Using RICM, DAPs were detected as zero-order black spots (4-12 nm separation from the surface) within a surrounding light gray-white membrane area (> 20 nm separation). A DAP, therefore, was the point of shortest distance between platelet membrane and immobilized VWF, which could be bridged by the GPIbα receptor protruding from the platelet surface.[23]

Platelet-derived tethers and microparticles in flow form through GPIbα-VWF interaction

With γ_w above 1000 s^{-1}, DAPs could remain stationary, at least temporarily, while the platelet body moved forward, forming membrane tethers up to 30 μm in length that maintained the continuity of the cell membrane (Figure 1B; Movie S1). Following the initial interaction of GPIbα with immobilized VWF, translocating platelets progressively became firmly attached to the surface and spread (Figure 1C; Movie S1) through a process dependent on integrin αIIbβ3 activation[6] (not shown). Blocking GPIbα or VWFA1 with specific monoclonal antibodies completely prevented platelet adhesion to VWF (not shown).[6] During the initial phase of transient adhesion, additional DAPs formed dynamically along the length of developing tethers, which could bend relative to the direction of flow and straighten after detachment of the DAP

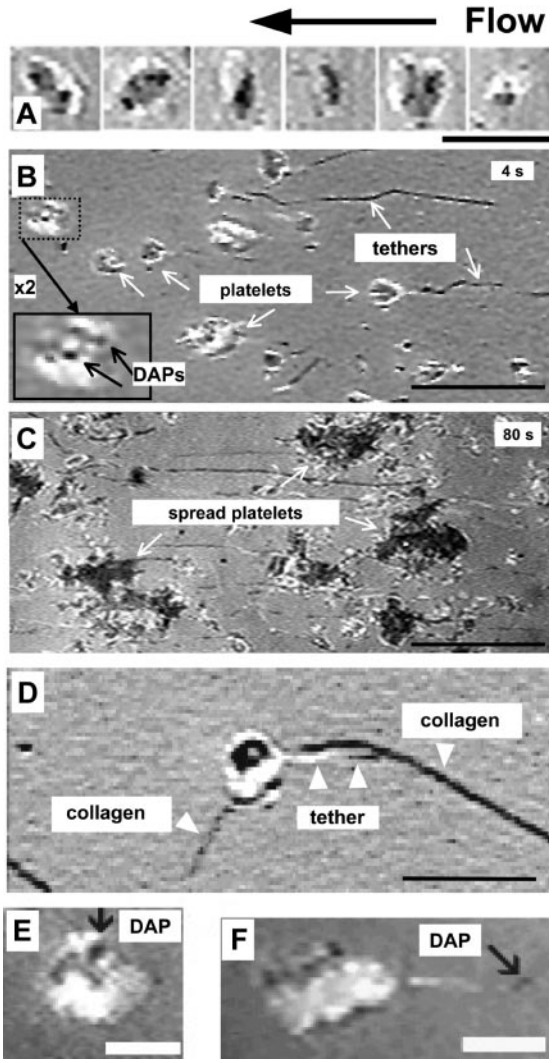

Figure 1. Platelet attachment, tether and PMP formation via DAPs. (A) Washed blood-cell suspension (platelet count, 11 000/μL) perfused over dVWFA1 at γ_w of 40 000 s^{-1}. Sequential frames of a platelet during translocation are shown from right to left: (1) initial membrane-dVWFA1 surface contact with few prominent DAPs (dark circular areas); (2) increase in the contact area and number of DAPs; (3) turn of bottom side up, with platelet seen on its edge (flip-roll motion); (4-6) sliding and rotation of the platelet body from right to left (translocation without rolling). Scale bar = 5 μm. See also Movies S1 and S5. (B) Whole blood containing PPACK perfused over immobilized VWF multimers at γ_w of 6 000 s^{-1}. After perfusion for 5 seconds, DAPs within the bodies of surface interacting platelets appear as dark areas (see enlarged inset), and tethers (some with pronounced kinks) extend from the body for variable lengths that may exceed 30 μm. Scale bar = 5 μm. (C) The same surface shown in panel B, but after perfusion for 80 seconds; spread platelets are visible. Scale bar = 10 μm. See Movie S1. (D) Washed blood-cell suspension with 20 μg/mL purified VWF perfused over collagen type I fibrils at γ_w of 4000 s^{-1}. The platelet count was reduced to 11 000/μL to decrease surface coverage, and 10 μM PGE_1 was added to prevent activation. A tethered platelet is seen during initial transient adhesion to collagen-bound VWF. Scale bar = 5 μm. See Movie S4. (E) Washed blood-cell suspension (230 000 platelets/μL) perfused over dVWFA1 at γ_w of 4000 s^{-1}. Note the attachment to the surface mediated by a DAP within the platelet body. Scale bar = 3 μm. See Movie S5. (F) Washed blood-cell suspension (270 000 platelets/μL) perfused over dVWFA1 at γ_w of 1000 s^{-1}. Note the attachment to the surface mediated by a DAP at the upstream end of a tether. Scale bar = 3 μm. (See Movie S6).

(Movie S2), as well as recoil when an upstream DAP lost surface contact (Movie S3). These findings are in agreement with those by Dopheide et al.[24] DAPs and tethers were also evident during platelet adhesion to collagen (Figure 1D; Movie S4), a relevant thrombogenic substrate of extracellular matrices[7] and atherosclerotic plaques.[25] Absolute requirement for platelet arrest onto

collagen was the binding of soluble VWF to the collagen fibrils (Movie S4).

The dynamic aspects of the initial platelet-surface contacts were studied using dVWFA1, which cannot support stable adhesion because it cannot interact with αIIbβ3. In experiments with γ_w ranging from a value found in normal arterioles (2000 s^{-1}) to a value found at points of lumen restriction in atherosclerotic coronary arteries (40 000 s^{-1}),[14,26,27] we observed that a single DAP positioned either within the platelet body or at the upstream end of a tether could be the only membrane area anchored to the surface. In the former cases it acted as a pivot during rotational or flip movements (Figure 1E; Movie S5); in the latter, it held the whole platelet body stationary (Figure 1F; Movie S6). Tethers only formed when low γ_w (< 1000 s^{-1}) was combined with low-coating concentrations of dVWFA1 (1 and 5 μg/mL) or when platelets interacting with dVWFA1 at higher coating concentrations (10-20 μg/mL) were exposed to higher γ_w (20 000-40 000 s^{-1}). In the latter case, more than 50% of arresting platelets formed tethers (Figure 2A-B). As measured by binding of a radiolabeled anti-VWFA1 monoclonal Fab (NMC-4), a function-blocking antibody,[28] coating concentrations of 10 or 20 μg/mL resulted in 60% or 85% maximal surface density of dVWFA1, respectively (mean of 2 experiments performed on different days). At saturation, we measured 125 NMC-4 Fab molecules bound per 0.05 μm^2 of surface (average of 3 separate experiments) which we assume to represent the functional density of VWFA1 sites potentially engaged by GPIbα in the smallest platelet DAP area found (measured by analysis of transmission electron microscopy images taken at 80 000-fold magnification).

Relative to total contact events, the number of platelets exhibiting continued translocation and forming tethered DAPs increased with increasing γ_w (Figure 2B). Tethered DAPs alternated between arrest and translocation but with longer stationary periods than the connected platelet bodies, resulting in an average velocity differential that allowed tethers to reach lengths of 30 μm in a few seconds (Figure 2C-D). At γ_w of 6000 s^{-1} and above, the main platelet body could detach from the tether, yielding a single tube-shaped platelet fragment that independently translocated on the surface (Figure 2E; Movie S7). At γ_w of 10 000 s^{-1} and above, the relative number of severed tethers increased, and, in addition, detached membrane fragments of less than half a micrometer in length appeared. These were actual platelet-derived microparticles, drop-like or spherical in shape, with diameters ranging from 50 to 100 nm (Figure 3) and continued to translocate on the VWF-coated surface independently of their platelets of origin (Movie S7). Although every platelet-VWF contact occurred via DAPs, not every arrest at γ_w exceeding 6000 s^{-1} resulted in tether and microparticle formation. Optimal shear rates for the event to occur were between 10 000 and 40 000 s^{-1} with an average 0.75:1:1 ratio of microparticles to isolated tethers to arresting platelets. Both PMPs and tethers exhibited the same diameter of 0.1 μm or less and were thus defined by their length (ie, microparticles below and tethers above 0.5 μm in length) (Figure 3A-E). On surface-coated collagen some tether formation occurred, but PMP generation was not significant (data not shown). As a control experiment we perfused whole blood at γ_w up to 40 000 s^{-1} over uncoated glass, to which plasma fibrinogen readily adsorbs.[29] In this case, platelet adhesion was absent, no tether and PMP generation occurred during flow, and no PMP increase could be detected in the perfused samples (data not shown).

GPIbα distribution in DAPs and tethers

To analyze the mechanism of tether and PMP formation in more detail, flow experiments were conducted over EM-grids and melamine-coated coverslips containing immobilized dVWFA1 at γ_w ranging from 10 000 to 30 000 s^{-1}. Dynamic events were captured during perfusion fixation. In scanning EM, thin membrane tethers were seen emerging from nonactivated platelets and were clearly distinct from the filopodia of activated platelets (Figure 3A-C). The morphology of severed tethers and microparticles (Figure 3D-E) confirmed the images seen with RICM in real time. Knoblike expansions, indicative of the DAPs seen during real-time visualization, were often located at the upstream ends of tethers but appeared also at distinct sites throughout their length. Immuno-EM analysis (Figure 3F-K) demonstrated that the GPIbα distribution along tethers was not uniform, as distinct areas with relative high GPIbα concentration alternated with regions exhibiting no GPIbα. Analysis of tilted (+10° and −10°) stereo pairs of immunogold-labeled DAPs revealed that GPIb was predominantly located at the DAPs' peripheral basolateral edges (toward the adhesive substrate) as compared with the luminal surface (data not shown). Bifurcations of membrane tethers presumably emerge from areas where DAPs interact with the dVWFA1 (Figure 3E). Thin-frozen sections of perfusion-fixed platelets following immunolabeling of GPIbα (Figure 4) revealed a distinct localization of the receptor at the narrow interface between the adhesive substrate and the platelet abluminal membrane. These sites likely represent the zero order black contact areas revealed by RICM, that is, the DAPs where tether formation is initiated (Figure 4A-C). The presence of GPIbα along thin membrane tethers was also apparent (Figure 4D-F).

Analysis of adhesion receptors and procoagulant molecules in platelet DAPs and tethers

Confocal microscopy analysis demonstrated that both microparticles and tethers exhibited on their surface the platelet receptor GPIbα and tissue factor, albeit the latter at low levels (Figure 5). The integrin αIIbβ3 was also detected (not shown). The presence

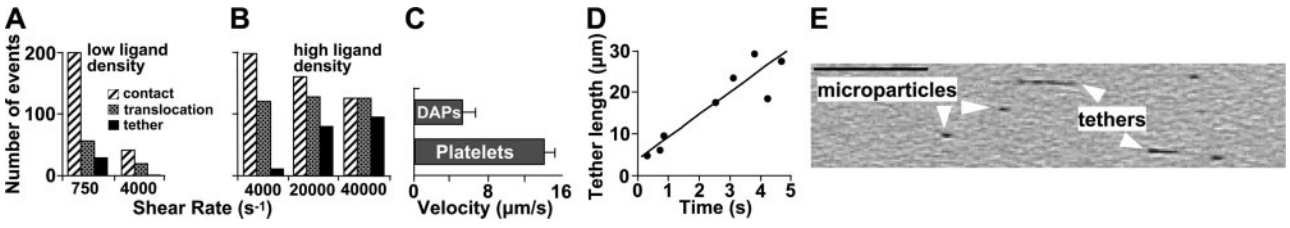

Figure 2. Kinetics of tether formation. (A-B) Washed blood-cell suspension (platelet count, 11 000/μL) perfused over immobilized dVWFA1 coated at low (A) or high (B) density (coating solution 1 or 20 μg/mL, respectively). Wall shear rates as shown. "Contact" indicates platelets interacting with the surface for at least 0.033 second; "translocation" specifies platelets moving on the surface by a distance more than 1 cell diameter in 2 seconds at lower than free-flow velocity; "tether" denotes platelets forming tethered DAPs. (C) Translocation velocity of platelets and their respective tethered DAPs. (D) Kinetics of tether formation at high dVWFA1 density and γ_w of 40 000 s^{-1}. (E) Washed blood-cell suspension with reduced platelet count (11 000 platelets/μL) perfused over dVWFA1 at γ_w of 40 000 s^{-1}. Isolated microparticles and tethers detached from platelets are seen while translocating on the surface. Scale bar = 5 μm. See Movie S7.

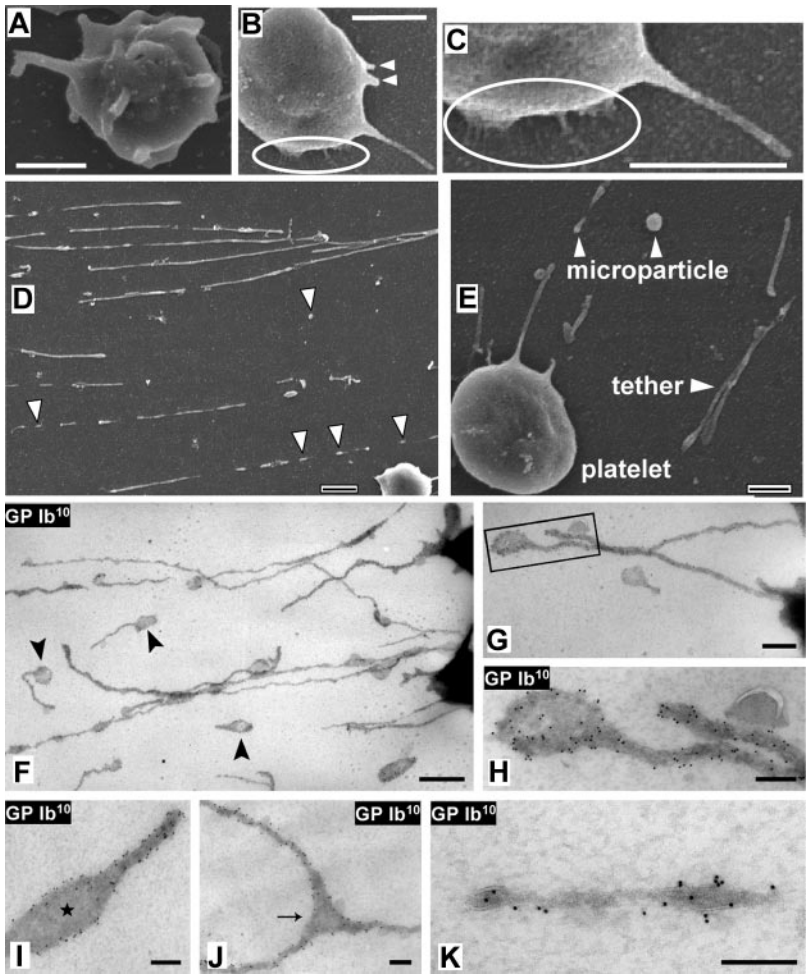

Figure 3. Scanning EM and whole-mount immuno-EM analysis of tethers and microparticles. (A-E) Citrated whole blood (platelet count, 250 000 platelets/μL) perfused over dVWFA1 at γ_w of 30 000 s^{-1}. (A) Scanning electron micrograph of a perfusion-fixed activated platelet, shown for comparison. The activated platelet shows multiple filopodia protruding from the surface in all directions. (B) A nonactivated platelet adhering to VWF through GPIbα. The membrane surface is smooth, and the long passively pulled tether has less than half the diameter of filopodia. Two short protruding membrane areas (arrowheads) are indicative of nascent tethers. (C) Enlargement of a detail highlighted in panel B, showing thin and short tethers connecting the platelet body to the adhesive substrate. (D-E) Isolated microparticles and detached tethers. Scale bars = 1 μm (A-D) or 0.5 μm (E). See Movie S7. (F-K) Citrated whole blood was perfused at γ_w of 30 000s^{-1} over dVWFA1-coated EM grids, fixed under flow, and immunolabeled with monoclonal anti-GPIbα antibody followed by protein A coupled to 10-nm gold particles ($GPIb^{10}$). (F-G) Severed tethers exhibiting tubular and globular domains, the latter (highlighted) corresponding to DAPs. (H-I) GPIbα in the globular tether end (DAP) is predominantly peripheral and excluded from the central zone. (J) Bifurcating tether showing peripheral GPIbα distribution in the DAP-like bifurcation zone (arrow). (K) Severed tubular tether exhibiting subdomains with variable GPIbα content. Scale bar in panel A = 1 μm; bar in panel B = 500 nm; bars in panels C to F = 200 nm.

of GPIbα explains the continued interaction of tethers and PMPs with immobilized VWF after separation from platelets. In agreement with EM data (Figure 3), immunofluorescence intensity variations along tethers and in PMPs revealed distinct subdomains with a higher GPIb density (Figure 5A). F-actin was readily detected in platelet bodies and, to some extent, also in microparticles and knoblike as well as thin tether ends (Figure 5B). No actin was detected in tethers and PMPs formed during flow of blood pretreated with cytochalasin D (Figure 5C-D). The leukocyte marker, CD14, was present at background levels on platelets (Figure 5E-F) and was not detected on tethers and microparticles. Staining for TF was present but at very low levels in platelets, tethers, and PMPs (compare Figure 5G-H).

Procoagulant function of PMPs generated by platelet exposure to high shear stress

In agreement with previous results,[8] a baseline amount of microparticles was present in normal blood samples (Figure 6A). Newly formed PMPs could be recovered in the blood flowing out of a

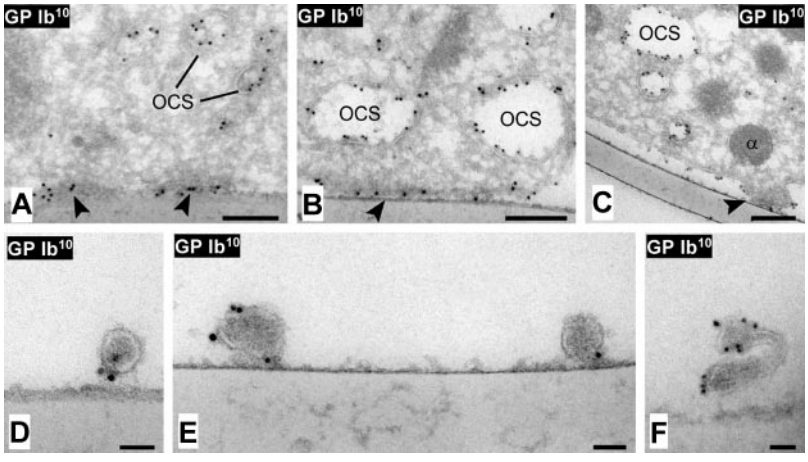

Figure 4. Immuno-EM analysis of cross-sectioned DAPs and tethers. Perfusions were carried out over melamine-plated coverslips coated with dVWFA1. Immunolabeling as described in the legend to Figure 3. The electron micrographs show DAPs of various sizes (A-C), and cross-sectioned tethers (D-F) attached to the dVWFA1 substrate. (A-B) DAPs appear in cross-section as darker areas of the membrane closely juxtaposed to the adhesive substrate and with high density of GPIbα (arrowheads); the latter is also detected in the open canalicular system (OCS). (C) A DAP (arrowhead) is in close contact with the adhesive substrate while the surrounding platelet membrane is lifting away, suggestive of a nascent tether or PMP. (D-F) Visualization of GPIbα in cross-sectioned tethers. Scale bar in panels A to C = 200 nm; bars in panels D to F = 50 nm.

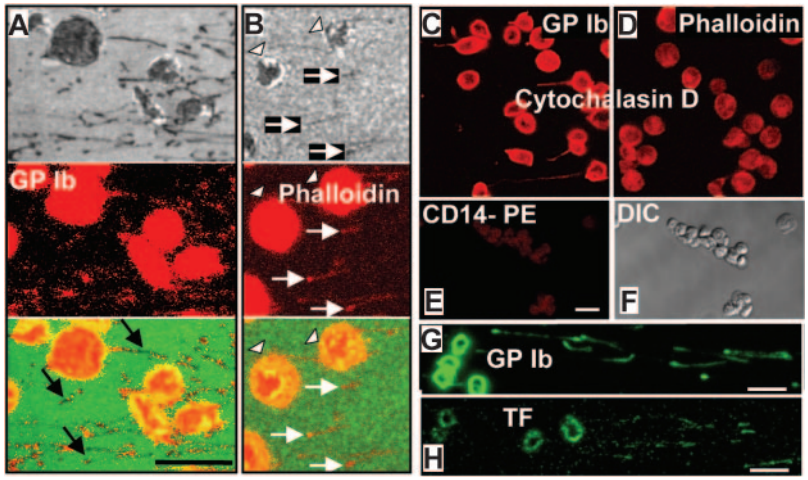

Figure 5. Immunofluorescence confocal microscopic analysis of GPIbα, F-actin, and tissue factor in perfusion-fixed tethers and microparticles. Whole blood was perfused over immobilized dVWFA1 at γ_w of 30 000 and 40 000 s^{-1}. (A-B) Two fields of view were visualized by RICM (top), confocal immunofluorescence microscopy after staining with an anti-GPIbα antibody (A) or phalloidin (B) to visualize F-actin (middle), and their composite (bottom). White arrows indicate microparticles and tethers; arrowheads show platelets. Phycoerythrin (PE) immunofluorescence staining for GPIbα (A) reveals abundant receptor exposure with a few unlabeled tether segments and microparticles (black arrows). This finding indicates a heterogeneous receptor distribution suggestive of clustering and corresponds well with the immuno-EM data in Figures 3 and 4. PE immunofluorescence staining for F-actin with phalloidin, despite the relatively low intensity (B), shows a complete congruence with the RICM image in the tether ends and microparticles. (C-D) Cytochalasin D–treated platelets clearly exhibit GPIbα labeling (Cy3), as do tethers and microparticles originating from them (C), whereas the phalloidin staining for F-actin (rhodamin) can be seen in platelets but is absent in tethers and microparticles (D). (E) The specific monocyte marker CD14 could not be detected on microparticles, tethers, and platelets, which exhibit only low background fluorescence. (F) Differential interference contrast (DIC) image of the field of view shown in panels E, G, and H. Comparative fluorescence staining (fluorescein) for GPIbα and tissue factor (TF) on microparticles, tethers, and platelets. Note the more intense staining with the anti-GPIbα antibody (G) as compared with the anti-TF antibody (H). All scale bars shown = 5 μm.

perfusion chamber after exposure to immobilized VWF and remained stable over several hours. The platelet count was not affected by the perfusion, but the number of PMPs in postperfusion samples increased 5.3- or 8.6-fold, respectively, depending on whether GPIbα or αIIbβ3 were used as platelet marker (Figure 6A). This discrepancy was due to a difference in preperfusion levels, as postperfusion microparticle counts were within 1%. Less than half of all the platelets detected before flow expressed low levels of tissue factor and showed a tendency to decrease in number after flow (not significant; Figure 6A). The count of PMP-expressing tissue factor increased 4.4-fold after flow, although only amounting to 44% of the microparticles positive for GPIbα or αIIbβ3 (Figure 6A). PMPs were measured by flow cytometry using gating parameters defined with microspheres of 0.1-μm diameter.

Quantitative and functional studies to address the issue of PMP procoagulant activity[30] were performed by subjecting platelets to shear stress in a cone-and-plate viscosimeter. PRP exposed to γ_w of 10 s^{-1} served as the baseline control. There was no significant increase in PMP number after PRP exposure to γ_w of 2000 or 6000 s^{-1}, but a 5.3-fold increase was found after shearing at γ_w of 10 000 s^{-1} (Figure 6B). When PRP was pretreated with cytochalasin D, the microparticle count after shearing at 10 000 s^{-1} was only 44% of that in untreated PRP (Figure 6C), indicating that the platelet cytoskeleton may regulate to some extent the effects of shear stress on PMP generation. In inverse correlation with the increase in PMP number, the clotting time of sheared PRP supplemented with calcium ions and TF shortened to 76% and 61% of baseline after exposure to γ_w of 6000 or 10 000 s^{-1}, respectively (Figure 6D). In other experiments, PPP was prepared from PRP exposed to shear stress before measuring the clotting time adding calcium ions but no TF. As compared with control samples exposed to γ_w of 10 s^{-1}, there was a significant shortening of the clotting time in the samples exposed to γ_w of 10 000 s^{-1} (Figure 6E), even though the absolute values were longer than in PRP supplemented with TF (compare Figure 6E with Figure 6D). The results obtained in the absence of platelets and without addition of exogenous TF indicate that PMPs generated by shear stress may have a direct procoagulant effect. Microscopic analysis of our samples suggested that flow cytometric evaluation was underestimating PMP counts, possibly because the small microparticles are not detected when entering the focus of the laser beam simultaneously with a platelet. The latter being more than 20 times larger in diameter gives a much stronger signal overriding the PMP signal. By increasing the concentration of the anti-CD41 antibody 11-fold and performing comparative analysis of PRP or PPP, we found that the rise in PMP counts above baseline was 16-fold and 55-fold, respectively (Figure 6F). These results were confirmed by evaluating the increase in PMPs that bound annexin V, which were 11-fold and 54-fold higher above baseline in PRP and PPP, respectively (Figure 6F). It appears, therefore, that platelets may mask small PMP during flow cytometric analysis, even though platelets and PMP are well differentiated by light-scattering properties (Figure 7). Of note, blocking the GPIbα-VWF interaction with the VWFA1 inhibitor NMC-4 Fab[28] entirely prevented PMP increases in samples exposed to γ_w of 10 000 s^{-1} (Figure 7), whereas blocking the integrin αIIbβ3 with tirofiban had no significant effect in this regard (not shown).

Discussion

Our studies define a quantal unit for platelet adhesion to immobilized VWF under fast flow conditions, which we have designated DAP (discrete adhesion point). High adhesion strength within a fully engaged DAP and tensile force resulting from hydrodynamic drag on adherent platelets create a mechanism for the generation of platelet-derived microparticles through cell-membrane disruption. This adaptive response may lead to the deposition on reactive vascular surfaces of procoagulant cell structures that, by virtue of their adhesive properties and small size, are not removed even under extreme flow conditions, for example, at the shear rates encountered in severely stenosed arteries.[31] DAPs, therefore, may

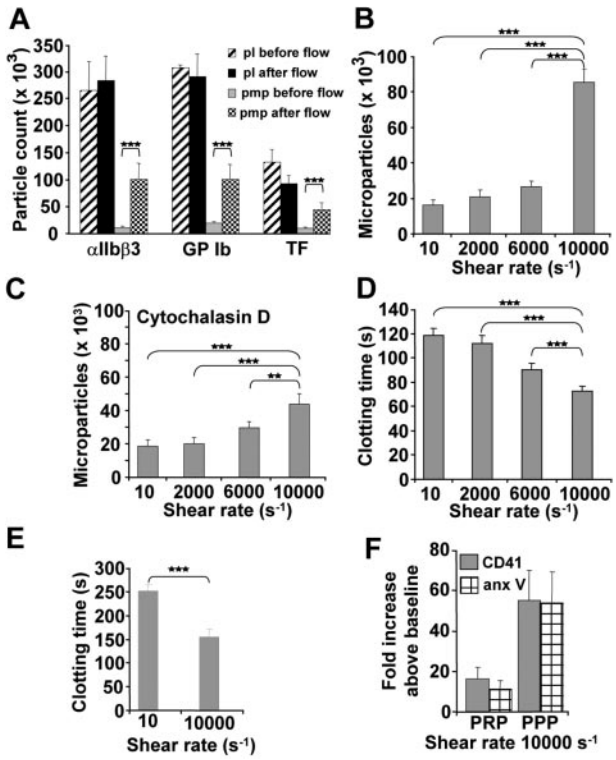

Figure 6. Flow cytometric analysis of shear-induced generation of procoagulant microparticles. (A) Increased microparticle but not platelet counts in citrated whole blood flowing out of a chamber after perfusion over dVWFA1 at γ_w of 30 000 s^{-1}. Flow cytometry was performed after centrifugation to PRP. Microparticles were identified by the presence of integrin αIIbβ3 (n = 5), GPIbα (n = 5), or tissue factor (TF; n = 9). Note that the microparticle counts with a positive TF signal were approximately half of the GPIb or αIIbβ3 positive ones. (B-C) Microparticle counts in citrated PRP exposed to different shear rates in a cone-and-plate viscosimeter (n = 4, respectively). Results obtained in control PRP (B) or PRP treated with cytochalasin D, which disrupts the actin cytoskeleton (C). In either case, the increase in microparticle generation was significant when γ_w of 10 000 s^{-1}. Note that the increase of microparticle counts in the cytochalasin D–treated PRP was approximately half that seen in control PRP. The counts reported in panels A to C are for events acquired over a 1-minute period (A) or a 3-minute period (B-C). (D) Clotting time obtained after addition of calcium ions (25 mM) and tissue factor (1.44 ng/mL) to PRP exposed to different shear rates (n = 8). A significant reduction was observed in PRP exposed to a shear rate of 10 000 s^{-1}. (E) Significant reduction of the clotting time obtained after addition of calcium but not tissue factor to PRP exposed to the shear rate of 10 000 s^{-1} (n = 3). PGE_1, apyrase, tirofiban, and CTI were present in the PRP. (F) Change in the number of microparticles positive for αIIbβ3 (CD41) or phosphatidylserine, measured by annexin (anx) V binding, after exposure of PRP to a shear rate of 10 000 s^{-1} (n = 5). The detected increase was more pronounced when the flow cytometric analysis after shearing was performed in PPP as compared with PRP. All results are shown as mean ± SEM. ***$P < .01$; **$P < .05$.

be important for platelet proadhesive and procoagulant functions in arterial thrombus formation.

Platelet tethering from rapidly flowing blood onto areas of vascular lesion appears to require the concurrent formation of multiple VWFA1-GPIbα bonds. For example, with γ_w of 10 000 s^{-1} the surface density of immobilized VWFA1 must be in the order of 1000 molecule/μm^2 to initiate platelet adhesion. This is the equivalent of 50 molecules in 0.05 μm^2 corresponding to the average contact area of a DAP. Assuming that 15 000 GPIbα receptors[32] are evenly distributed[33] on a nonactivated platelet with an average surface area of 10 μm^2 (calculated for a spread platelets leaving no membrane hidden in the open canalicular system), a DAP of 0.05 μm^2 may contain at least 75 GPIbα molecules. This number may be increased by receptor clustering, as demonstrated by our immuno-EM results, which may be required to support platelet adhesion at the shear rates that develop at the tip of growing thrombi in the arterial circulation.[19] In any case, the calculated number of GPIbα receptors in a DAP matches well the functional density of VWFA1 required for platelet surface arrest in rapidly flowing blood. In a flow field with γ_w of 40 000 s^{-1} a DAP may oppose a force of 160 pN, but this corresponds to only 1.6 pN per bond if 100 bonds are formed concurrently. The latter value is of the same order of magnitude as the adhesive strength of 6.5 to 8.8 pN calculated for a single VWF-GPIbα bond from the force required to detach VWF-coated beads from GPIbα-expressing Chinese hamster ovary cells.[34] This is in contrast to a single P selectin ligand bond, reportedly sufficient for leukocyte arrest at low venous shear rates, capable of resisting a tensile force of 112 pN.[35] The distribution of high adhesive forces over multiple bonds may be a unique requirement for platelets, which must function in arterial flow, and DAPs may represent the structural unit for the coordination of multivalent GPIbα-VWFA1 interactions.

The cumulative adhesive strength of one or more DAPs can oppose fluid dynamic drag, at least temporarily, and hold a platelet stationary on a surface. Eventually, hydrodynamic forces may overcome membrane tension[36,37] and cause a forward movement of the platelet body, if devoid of other sites of tight surface attachment, while still tethered to the arrested DAP. It is not clear why

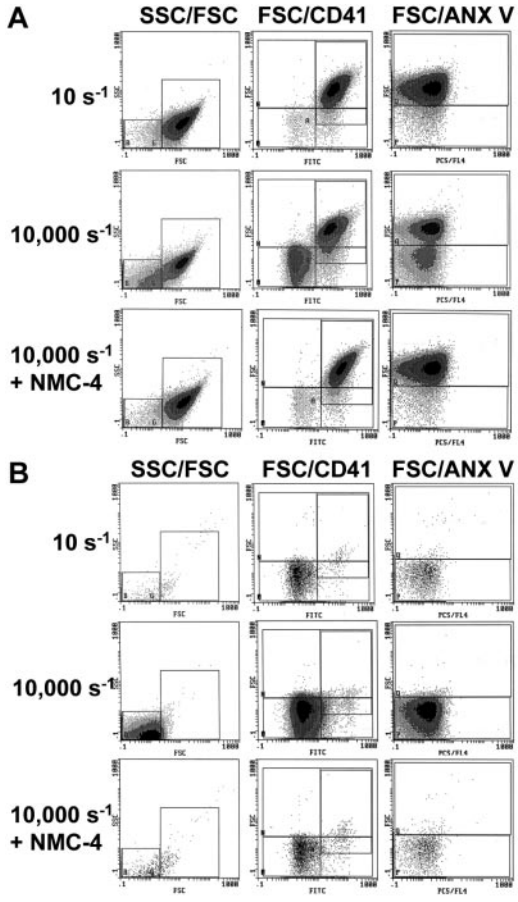

Figure 7. Dependency of shear-induced PMP generation on the GPIb-VWF interaction. Flow cytometric analysis was performed after exposure of citrated PRP to shear rates of 10 s^{-1} or 10 000 s^{-1} in a cone-and-plate viscosimeter. In all samples, platelet activation and aggregation was blocked by addition of PGE_1, apyrase, and tirofiban. Flow cytometric analysis was performed in PRP (A) or PPP (B). Samples were double-labeled with fluorescein isothiocyanate–conjugated anti-CD41 to show platelet specificity and with phycoerythrin-Cy5–conjugated annexin V to determine phosphatidyl serine expression. Exposure to high shear rates increased PMPs with phosphatidyl serine membrane expression. Blocking the GPIb-VWF interaction with NMC-4 completely inhibited generation of PMP.

only limited areas of the platelet membrane display maximal adhesion to VWF. Resting platelets have a smooth outer surface[38] and bear no structure comparable to the leukocyte microvilli that promote rolling through selectins and their ligands.[39] As a possible explanation, DAPs may contain selectively distributed clusters of GPIbα molecules dissociated from the membrane skeleton, a condition reported to result in enhanced VWF binding.[40,41] Tensile force applied on these receptors is transferred to membrane not reinforced by actin. Consequently, when the elasticity module of the membrane is overcome at shear rates exceeding 6000 s^{-1}, tethers are extruded and eventually severed. Passive deformation of the membrane surrounding GPIbα receptors in a DAP may contribute to adhesion by decreasing the force acting on the bonds and prolonging the duration of interactions while preserving cellular integrity. Nonetheless, without anchoring to the cytoskeleton, the tethering membrane may be severed more easily before DAP detachment. Thus, properties that favor platelet adhesion to VWF may also lead to microparticle generation. Tethers contained low amounts of F-actin but their formation velocity at an average rate of 1 μm per 50 to 150 milliseconds was up to 7 times faster than actin can polymerize.[42] Although morphologically similar, therefore, tethers being passively pulled from the membrane are distinct from filopodia actively protruding through intracellular actin polymerization following platelet stimulation.

F-actin can be detected in DAPs, but its relative paucity in tethers may be one reason for their formation. This is corroborated by the fact that blocking actin polymerization and depolymerizing already present actin filaments with cytochalasin D still allowed tether formation in platelets adhering to VWF and tripled the maximum tether length obtained in an equivalent time interval (not shown). These findings, which are in agreement with a previous report,[24] suggest some preventive role for F-actin in tether elongation. However, shear-induced PMP formation was reduced with cytochalasin treatment of platelets. A conceivable explanation is that cytochalasin D increases the portion of membrane dissociated from the cytoskeleton, while severing of tethers with PMP generation may occur more readily at sites of membrane-cytoskeleton linkage subjected to shear stress. However, the size of PMP observed in our study appears to be independent of cytoskeletal integrity and may be determined by the area of the DAP membrane extruded and severed from the platelet.

Although tether formation dependent on GPIbα interaction with immobilized VWF was described earlier,[24] the process of shear-induced generation of isolated tethers and microparticles had not been visualized in detail. Moreover, our studies now indicate that the same mechanism leading to platelet microparticle formation at an immobilized VWF surface may take place when VWF is bound to the membrane of platelets exposed to fluid shear stress in suspension. Such a conclusion is supported by the observation that the shear rate threshold for PMP formation is essentially the same, between 6000 s^{-1} and 10 000 s^{-1}, whether platelets adhere to immobilized VWF or to one another in the absence of aggregation. In either situation, the mechanical shedding of PMPs is completely dependent on the interaction of GPIbα with VWF, independent of platelet activation and aggregation, and distinct from proteolytic shedding, which unlike the process described here requires calcium. Thus, our data agree with the conclusion[8] that microparticle formation influenced by soluble VWF is mediated by GPIbα, and not by integrin αIIbβ3, as found by others.[9] A possible explanation for the discrepancy may be the use of washed platelets in buffer,[9] as opposed to platelet-rich plasma in our experiments, which may have limited the availability of VWF. Furthermore, a flow cytometric definition of microparticles as being smaller than platelets[9] may identify different structures than the ones we visualized as having a diameter of 0.05 to 0.1 μm and for which we calibrated our flow cytometric gating.

PMPs retained an intrinsic adhesive function and supported thrombin generation, probably because of their expression of phosphatidylserine. Whether the tissue factor we detected at low levels on platelets and PMPs was in an active decrypted or encrypted form, and thus played any role in thrombin generation, could not be discerned with the antibodies we used. Contrary to others, we found no evidence for a monocytic origin of the TF.[13,43] Thrombin generation has also been described as being promoted by microparticles from healthy individuals in the presence of inhibitory antibodies to tissue factor, factor VII, and factor XII.[44] Our real-time studies, therefore, suggest that regions in the vasculature exhibiting high shear rates and immobilized VWF, such as the luminal surface of an obstructing atherosclerotic plaque, could trigger the generation of procoagulant microparticles via platelet GPIbα-VWF interactions.

Acknowledgments

We thank Jerry Ware for helpful discussion; James R. Roberts and Richard A. McClintock for the preparation of VWF fragments; Jennifer Orje and Rolf Habermann for help with flow experiments and movie production, respectively; Rachel Braithwaite for secretarial assistance; Helga Wehnes for expert technical assistance with SEM; and Bernd Engelmann for generous access to the cone-and-plate device. There is no conflict of interest for any of the authors with regard to this manuscript or the work contained therein. This work is part of the thesis of H.S.

References

1. Ruggeri ZM. Platelets in atherothrombosis. Nat Med. 2002;8:1227-1234.
2. Goldsmith HL, Mason SG. Axial migration of particles in poiseuille flow. Nature. 1961;190:1095-1096.
3. Goldsmith HL, Cokelet G, Gaehtgens P. Robin Fahraeus: evolution of his concepts cardiovascular physiology. Am J Physiol. 1989;257:H1005-H1015.
4. Weiss HJ. Flow-related platelet deposition on subendothelium. Thromb Haemost. 1995;74:117-122.
5. Farndale RW, Sixma JJ, Barnes MJ, De Groot PG. The role of collagen in thrombosis and hemostasis. J Thromb Haemost. 2004;2:561-573.
6. Savage B, Saldivar E, Ruggeri ZM. Initiation of platelet adhesion by arrest onto fibrinogen or translocation on von Willebrand factor. Cell. 1996; 84:289-297.
7. Savage B, Almus-Jacobs F, Ruggeri ZM. Specific synergy of multiple substrate-receptor interactions in platelet thrombus formation under flow. Cell. 1998;94:657-666.
8. Miyazaki Y, Nomura S, Miyake T, et al. High shear stress can initiate both platelet aggregation and shedding of procoagulant containing microparticles. Blood. 1996;88:3456-3464.
9. Haga JH, Slack SM, Jennings LK. Comparison of shear stress-induced platelet microparticle formation and phosphatidylserine expression in presence of αIIbβ3 antagonists. J Cardiovasc Pharmacol. 2005; 41:363-371.
10. Heijnen HF, Schiel AE, Fijnheer R, Geuze HJ, Sixma JJ. Activated platelets release two types of membrane vesicles: microvesicles by surface shedding and exosomes derived from exocytosis of multivesicular bodies and alpha-granules. Blood. 1999;94:3791-3799.
11. Biro E, Sturk-Maquelin KN, Vogel GMT, et al. Human cell-derived microparticles promote thrombus formation in vivo in a tissue factor-dependent manner. J Thromb Haemost. 2003; 1:2561-2568.
12. Müller I, Klocke A, Alex M, et al. Intravascular tissue factor initiates coagulation via circulating microvesicles and platelets. FASEB J. 2003;17:476-478.
13. Falati S, Liu Q, Gross P, et al. Accumulation of

tissue factor into developing thrombi in vivo is dependent upon microparticle P-selectin glycoprotein ligand 1 and platelet P-selectin. J Exp Med. 2003;197:1585-1598.

14. Mailhac A, Badimon JJ, Fallon JT, et al. Effect of an eccentric severe stenosis on fibrin(ogen) deposition on severely damaged vessel wall in arterial thrombosis: relative contribution of fibrin(ogen) and platelets. Circulation. 1994;90: 988-996.
15. Siegel JM, Markou CP, Ku DN, Hanson SR. A scaling law for wall shear rate through an arterial stenosis. J Biomech Eng. 1994;116:446-451.
16. Bluestein D, Niu L, Schoephoerster RT, Dewanjee MK. Fluid mechanics of arterial stenosis: relationship to the development of mural thrombus. Ann Biomed Eng. 1997;25:344-356.
17. Curtis ASG. The mechanism of adhesion of cells to glass. A study by interference reflection microscopy. J Cell Biol. 1964;20:199-215.
18. Kloboucek A, Behrisch A, Faix J, Sackmann E. Adhesion-induced receptor segregation and adhesion plaque formation: a model membrane study. Biophys J. 1999;77:2311-2328.
19. Ruggeri ZM, Dent JA, Saldivar E. Contribution of distinct adhesive interactions to platelet aggregation in flowing blood. Blood. 1999;94:172-178.
20. Ruggeri ZM, De Marco L, Gatti L, Bader R, Montgomery RR. Platelets have more than one binding site for von Willebrand factor. J Clin Invest. 1983;72:1-12.
21. Azuma H, Hayashi T, Dent JA, Ruggeri ZM, Ware J. Disulfide bond requirements for assembly of the platelet glycoprotein Ib binding domain of von Willebrand factor. J Biol Chem. 1993;268:2821-2827.
22. Heynen H, Lozano Molero M, De Groot PG, Nieuwenhuis HK, Sixma JJ. Absence of ligands bound to glycoprotein IIb-IIIa on the exposed surface of a thrombus may limit thrombus growth in flowing blood. J Clin Invest. 1994;94:1098-1112.
23. Lopez JA, Andrews RK, Afshar-Kharghan V, Berndt MC. Bernard-Soulier syndrome. Blood. 1998;91:4397-4418.
24. Dopheide SM, Maxwell MJ, Jackson SP. Shear-dependent tether formation during platelet translocation on von Willebrand factor. Blood. 2002;99: 159-167.
25. Penz S, Reininger AJ, Brandl R, et al. Human atheromatous plaques stimulate thrombus formation by activating platelet glycoprotein VI. FASEB J. 2005;19:898-909.
26. Bathe M, Kamm RD. A fluid-structure interaction finite element analysis of pulsatile blood flow through a compliant stenotic artery. J Biomech Eng. 1999;121:361-369.
27. Wootton DM, Markou CP, Hanson SR, Ku DN. A mechanistic model of acute platelet accumulation in thrombogenic stenoses. Ann Biomed Eng. 2001;29:321-329.
28. Celikel R, Varughese KI, Madhusudan, Yoshioka A, Ware J, Ruggeri ZM. Crystal structure of the von Willebrand factor A1 domain in complex with the function blocking NMC-4 Fab. Nat Struct Biol. 1998;5:189-194.
29. Reininger AJ, Agneskirchner J, Bode P, Spannagl M, Wurzinger LJ. c7E3 Fab inhibits low shear flow modulated platelet adhesion to endothelium and surface-adsorbed fibrinogen by blocking platelet GP IIb/IIIa as well as endothelial vitronectin receptor: results from patients with acute myocardial infarction and healthy controls. Thromb Haemost. 2000;83:217-223.
30. Sims PJ, Wiedmer T, Esmon CT, Weiss HJ, Shattil SJ. Assembly of the platelet prothrombinase complex is linked to vesiculation of the platelet plasma membrane. Studies in Scott syndrome: an isolated defect in platelet procoagulant activity. J Biol Chem. 1989;264:17049-17057.
31. Holme PA, Orvim U, Hamers MJ, et al. Shear-induced platelet activation and platelet microparticle formation at blood flow conditions as in arteries with a severe stenosis. Arterioscler Thromb Vasc Biol. 1997;17:646-653.
32. Coller BS, Peerschke EI, Scudder LE, Sullivan CA. Studies with a murine monoclonal antibody that abolishes ristocetin-induced binding of von Willebrand factor to platelets: additional evidence in support of GP Ib as a platelet receptor for von Willebrand factor. Blood. 1983;61:99-110.
33. White JG, Krumwiede MD, Escolar G. Glycoprotein Ib is homogeneously distributed on external and internal membranes of resting platelets. Am J Pathol. 1999;155:2127-2134.
34. Arya M, Anvari B, Romo GM, et al. Ultralarge multimers of von Willebrand factor form spontaneous high-strength bonds with the platelet glycoprotein Ib-IX complex: studies using optical tweezers. Blood. 2002;99:3971-3977.
35. Alon R, Hammer DA, Springer TA. Lifetime of the P-selectin-carbohydrate bond and its response to tensile force in hydrodynamic flow. Nature, 1995; 374:539-542.
36. Raucher D, Sheetz MP. Characteristics of a membrane reservoir buffering membrane tension. Biophys J. 1999;77:1992-2002.
37. Shao JY, Ting-Beall HP, Hochmuth RM. Static and dynamic lengths of neutrophil microvilli. Proc Natl Acad Sci U S A. 1998;95:6797-6802.
38. George JN, Colman RW. Overview of platelet structure and function. In: Colman RW, Hirsh J, Marder VJ, Clowes AW, George JN, eds. Hemostasis and Thrombosis: Basic Principles and Clinical Practice. Philadelphia: Lippincott, Williams and Wilkins; 2001:381-386.
39. von Andrian UH, Hasslen SR, Nelson RD, Erlandsen SL, Butcher EC. A central role for microvillous receptor presentation in leukocyte adhesion under flow. Cell. 1995;82:989-999.
40. Fox JE. Linkage of a membrane skeleton to integral membrane glycoproteins in human platelets. Identification of one of the glycoproteins as glycoprotein Ib. J Clin Invest. 1985;76:1673-1683.
41. Englund GD, Bodnar RJ, Li Z, Ruggeri ZM, Du X. Regulation of von Willebrand factor binding to the platelet glycoprotein Ib-IX by a membrane skeleton-dependent inside-out signal. J Biol Chem. 2001;276:16952-16959.
42. Pollard TD, Blanchoin L, Mullins RD. Biophysics of actin filament dynamics in nonmuscle cells. Annu Rev Biophys Biomol Struct. 2000;29:545-576.
43. Del Conde I, Shrimpton CN, Thiagarajan P, López JA. Tissue-factor–bearing microvesicles arise from lipid rafts and fuse with activated platelets to initiate coagulation. Blood.2005;106:1604-1611.
44. Nieuwland R, Sturk A. Platelet derived microparticles. In: Michelson AD, ed. Platelets. San Diego: Academic Press; 2002:255-265.